

RESEARCH ARTICLE OPEN ACCESS

Use of the Calibrated Curve Number and a Runoff-Driven USLE Model to Estimate Event Soil Loss From Sparacia (Sicily, Southern Italy) Plots

Vincenzo Pampalone¹  | Dario Autovino¹ | Maria Angela Serio¹  | Vincenzo Bagarello¹  | Vito Ferro^{1,2} 

¹Department of Agricultural, Food and Forest Sciences, University of Palermo, Palermo, Italy | ²NBFC, National Biodiversity Future Center, Palermo, Italy

Correspondence: Maria Angela Serio (mariaangela.serio@unipa.it)

Received: 27 December 2024 | **Revised:** 27 June 2025 | **Accepted:** 3 July 2025

Funding: This study was carried out within the RETURN Extended Partnership and received funding from the European Union Next-GenerationEU (National Recovery and Resilience Plan-NRRP, Mission 4, Component 2, Investment 1.3–D.D. 1243 2/8/2022). This study was also carried out within the PRIN 2022 “Soil Conservation for sustainable Agriculture in the framework of the European green deal” (SCALE), Project code 2022PB2NSP, CUP B53D23017980006 and received funding from the European Union Next-GenerationEU (National Recovery and Resilience Plan-NRRP, Mission 4, Component 2, Investment 1.1).

Keywords: CN method | erosion plot | event soil loss | event-based runoff | plot runoff | USLE-based models

ABSTRACT

The Natural Resources Conservation Service (NRCS)-curve number (CN) method was originally proposed to predict runoff on small and midsize catchments, but it has also been used at the scale of erosion plots. In this case, uncertainties exist with reference to the factors, for example, scale effects, affecting the experimental CN values. In this study, the reliability of the CN method in reproducing plot runoff is analysed by using data collected at the Sparacia erosion plots (Sicily, Southern Italy), which are characterised by different sizes and steepness. This investigation aimed to test the possibility of using simulated runoff within universal soil loss equation (USLE)-type models, including runoff as a term in the erosivity factor. This analysis pointed out that the experimentally determined value of the initial abstraction ratio of the CN method was very low (0.0001). For each plot type (i.e., fixed length and steepness), the calibration was performed for 18 combinations of three rainfall ranges (all data, rainfall depth less than the median, and exceeding the median), two calibration approaches (least-squares and median value) and three datasets (all data, interrill, and rill). The best CN model fit was systematically produced for data with rainfall depth less than the median. The least-squares calibration approach generally performed slightly better than the median value one. Results showed that the CN method can be considered effective only for events producing rills. The CN values generally increased with plot steepness and decreased as plot length increased. For each plot type, CN tendentially increased for increasing soil moisture before the rainfall event, but moisture and rainfall depth were able to explain a minor part (from 19.5% to 41%) of CN variance. Finally, the USLE-MB that incorporates runoff simulated by the CN method was found to satisfactorily predict (relative standard error = 0.69, Nash and Sutcliffe Efficiency Index = 0.54) event soil loss caused by simultaneous interrill and rill erosion due to the higher rainfall depths recorded at the Sparacia station.

1 | Introduction

Predicting plot soil loss at the event temporal scale is necessary to design effective soil conservation measures since a large

proportion of total soil erosion over a long time period is due to a relatively few large storms (Edwards and Owens 1991; Larson et al. 1997; Bagarello et al. 2010b; Bagarello, Di Stefano, et al. 2011; Pampalone and Ferro 2020). Due to its relative

This is an open access article under the terms of the [Creative Commons Attribution](https://creativecommons.org/licenses/by/4.0/) License, which permits use, distribution and reproduction in any medium, provided the original work is properly cited.

© 2025 The Author(s). *Hydrological Processes* published by John Wiley & Sons Ltd.

simplicity, empirical modelling of the soil erosion process is attractive from a practical point of view (Cao et al. 2015; Gessesse et al. 2015; Bagarello, Ferro, and Flanagan 2018). However, the empirical approach has been questioned by different researchers since the physics of the process is not accurately described and empirical models are strictly valid with reference to the calibration environments (Morgan 2005; Boardman 2006). On the other hand, process-oriented models simulate different hydrological (infiltration and runoff) and erosive (soil detachment, transport and deposition) components of the erosion process, but some doubts and difficulties arise from both the used equations and the parameter estimation (Bagarello, Ferro, and Flanagan 2018). For example, the interrill erodibility, which is a key parameter in the Water Erosion Prediction Project (WEPP) model, ignores the influence of the soil structure, especially the aggregate stability that affects soil susceptibility to raindrop detachment (Liu et al. 2023). Pragmatically, empirical and process-oriented models constitute a complementary suite of models to be chosen to meet the specific user need (Nearing 2013; Bagarello, Ferro, and Flanagan 2018). Consequently, the empirical approaches of soil loss prediction continue to receive interest from the scientific community (Kinnell 2019, 2023; Bagarello et al. 2020).

The universal soil loss equation (USLE) (Wischmeier and Smith 1978) represents the most widely used empirical soil loss prediction model. Although the USLE was not designed to predict short-term soil losses (Ferro 2010), this equation has represented the basis to develop variants usable at the event temporal scale. In this context, an empirical approach that seems promising to estimate event soil loss makes use of an erosivity index given by the combination of the event runoff coefficient, Q_R (–), and the single-storm erosion index, EI_{30} ($\text{MJ mm ha}^{-1} \text{h}^{-1}$). I_{30} (mm h^{-1}) is the maximum 30-min rainfall intensity and E (MJ ha^{-1}) is the rainfall energy calculated according to Wischmeier and Smith (1978) starting from the rainfall kinetic energy per unit volume of rainfall and unit area (Carollo et al. 2018; Serio et al. 2019).

In particular, using the $Q_R EI_{30}$ term as the erosivity index, the so-called USLE-M model was empirically derived (Kinnell and Risse 1998; Kinnell 2007, 2010). Bagarello et al. (2008, 2010b, 2013, 2015b); Bagarello et al. (2010a) proposed a modified version of the USLE-M, named USLE-MM, in which the $Q_R EI_{30}$ term was raised to a power, b_1 , greater than one. In the more recently proposed USLE-MB (Bagarello, Di Stefano, et al. 2018; Pampalone et al. 2018; Di Stefano et al. 2019), the erosivity index was still defined by considering both Q_R and EI_{30} , but only the former term was raised to an exponent b_1 greater than 1. The USLE-MM and USLE-MB models were developed on data collected on bare plots established at the Sparacia experimental station for soil erosion measurement in Sicily, South Italy (Pampalone et al. 2022). A recent study (Pampalone et al. 2023) revealed an increased predictive ability of the USLE-MB when differently parameterised for rill + interrill and interrill data, that is, using events with simultaneous rill and interrill erosion or events with the single interrill component. The USLE-MB parameterised with rill + interrill data is given by the following Equation (1):

$$A_e = Q_R^{1.012} EI_{30} 0.334 \left(\frac{l}{22} \right)^\alpha 190.27 [\exp(0.06s) - 1] \quad (1)$$

where A_e (t ha^{-1}) is plot soil loss at the event scale, l (m) is the plot length, s (–) is the plot steepness, and $\alpha = 0.58$ for $11 \leq l \leq 22$ m and $\alpha = 0$ for $22 \leq l \leq 44$ m. The exponent $b_1 = 1.012$ practically coincides with that of the USLE-M ($b_1 = 1$).

Event soil loss prediction by the mentioned variants of the USLE requires an estimation of the event runoff (Yu et al. 1997; Vandervaere et al. 1998; Todisco et al. 2015). Runoff should be estimated with a simple method, especially in terms of input data, not to make event soil loss prediction nearly impossible in practise.

With reference to this last point, a step forward that could be made is to couple any variant of the USLE with the Natural Resources Conservation Service (NRCS) curve number (CN) method (SCS 1985, 1993), as suggested by Gao et al. (2012).

This method is based on the following equations:

$$\begin{cases} Q = \frac{(P - \lambda S)^2}{P + (1 - \lambda)S} & \text{if } P - \lambda S > 0 \\ Q = 0 & \text{otherwise} \end{cases} \quad (2)$$

where Q (mm) is the runoff volume per unit plot surface, P (mm) is the total precipitation depth, λ is the initial abstraction ratio and S (mm) is the maximum potential retention. The CN is related to S as:

$$CN = \frac{25400}{S + 254} \quad (3)$$

and varies from 1 to 100, with larger CNs estimating higher runoff.

From a practical point of view, coupling USLE variants and CN method appears reasonable since the latter should be characterised by a remarkable simplicity of application as the main runoff producing characteristics, including soil type, land use/treatment, surface conditions and soil moisture conditions, are incorporated into a single parameter (Ponce and Hawkins 1996). In other terms, runoff estimation would not represent an obstacle to soil erosion estimation. According to Ponce and Hawkins (1996), simplicity, that is linked to the conceptual nature of the method (Branson et al. 1962, 1981), does not imply necessarily an inferiority of the CN method as compared with more complex physically based methods. Accuracy of the CN method in estimating runoff depth (Ponce and Hawkins 1996) can depend on several factors, including (i) the marked sensitivity of the predicted runoff to curve number, (ii) the circumstance that the determination of the antecedent moisture condition is left to the user without any guide, (iii) the method is applied to sites different from that of the original deduction (range and forest types), and (iv) an abstraction ratio different from the original standard value of 0.2 is used to consider the variability due to different geologic and climatic settings (Bosznay 1989).

The CN method has also been adopted by many hydrological models to determine runoff, such as Chemical Runoff and Erosion from Agricultural Management Systems (CREAMS) (Knisel 1980), Areal Nonpoint Source Watershed Environment Response Simulation (ANSWERS) (Beasley et al. 1980), Agricultural Non-Point Source (AGNPS) (Young et al. 1989),

Erosion Productivity Impact Calculator (EPIC) (Sharpley and Williams 1990) and Soil and Water Assessment Tool (SWAT) (Neitsch et al. 2005).

Of course, a consequence of the mentioned simplicity of the CN approach is that some of the factors that influence rainfall-runoff transformation are described only approximately or are totally ignored, and the method, working in the mean, describes average trends (Ponce and Hawkins 1996). In other words, the CN approach does not consider the spatial and temporal variability of infiltration and abstraction rates and gives average runoff estimates accordingly. A conceptual implication of this circumstance is that coupling the CN method with a variant of the USLE should yield an estimate of the mean value of the event soil loss that can locally occur under a given hydrological forcing. In other terms, the predicted soil loss will be the expected mean event soil loss when the area of interest is subjected to a fixed rainfall depth value for a large number of times. Testing this concept as well as assumptions and simplifications of the CN method could help to improve the representation of these average trends.

The CN method has no explicit provision for spatial scale effects and it is assumed to apply to small and midsize catchments (Ponce and Hawkins 1996). However, it has also been used at the plot scale (e.g., Huang et al. 2006, 2007; Fu et al. 2011; Gao et al. 2012; Lal et al. 2015; Shi et al. 2018). The effects of plot length and steepness on total runoff are not considered by the CN method although these effects on event surface runoff have been widely documented in the literature (e.g., Evett and Dutt 1985; Chaplot and Le Bissonnais 2000; Bagarello et al. 2015a; Bagarello and Ferro 2017). Sharpley and Williams (1990) included an empirical slope factor into the CN method but subsequent investigations (Huang et al. 2006; Lal et al. 2015) demonstrated that this slope factor did not improve runoff prediction, if not marginally, in other environments. Consequently, alternative methods to take steepness effects into account were suggested (Huang et al. 2006; Lal et al. 2015), but due to the empirical origin of these methods they cannot be considered usable in other sites without testing. Moreover, there seems to be little or nothing regarding the link between the CN and the plot length. In the recent past, data from plots of different length were averaged starting from the premise that the CN model cannot take the effect of plot length into account (Gao et al. 2012).

To describe the soil water content conditions before a runoff event, the CN method commonly uses three discrete levels of soil antecedent moisture, AMC, defined by the 5 days antecedent rainfall depth. The use of three discrete levels implies a sudden jump in the CN value from one level to another (Hawkins 1978). Hawkins et al. (1985) interpreted the AMC categories as envelopes indicating the experienced variability in rainfall-runoff data, and Ponce and Hawkins (1996) suggested that site moisture acts as a surrogate for all other sources of variability, beyond that which could be attributed to soil, land use/treatment, and surface condition. In this perspective, antecedent rainfall could not describe well antecedent moisture effects that instead have to be established locally, as also demonstrated by Huang et al. (2007) and Lal et al. (2015).

Another factor to be considered is initial abstraction, that is the amount of rainfall abstracted as interception, infiltration and

surface storage before runoff begins (Ponce and Hawkins 1996). This initial abstraction is described as a fixed fraction, λ , of potential retention, S (Equation 2). The standard value is $\lambda=0.2$ but a wide range of values ($0 < \lambda \leq 0.49$) has been reported in the literature (Ponce and Hawkins 1996; Hawkins et al. 2002; Fu et al. 2011; Assaye et al. 2021). According to Lal et al. (2015), the standard λ value can be too high at the plot scale and values of 0–0.03 could be more appropriate. Moreover, λ can also be expected to vary with the antecedent moisture (Mishra et al. 2006).

According to Ponce and Hawkins (1996), the CN method could better describe runoff generation due to the saturation overland flow mechanism as compared with the Hortonian one. The accuracy of the predicted event runoff with the CN method could depend (Fu et al. 2011; Moglen et al. 2022) on the event rainfall depth. A given area could respond differently in terms of the experimentally obtained CN value depending on the rainfall characteristics (intensity, duration, spatial variability, rainfall event threshold) of the hydrological forcing (Chin 2023; Moglen et al. 2023). Translating this reasoning into the field of erosive phenomena that depend on this hydrological forcing, it cannot be excluded that the CNs could vary with rainfall erosivity or with the prevailing soil erosion mechanism such as, for example, only interrill or rill plus interrill. Support for this hypothesis can be found in Bagarello, Ferro, et al. (2011) since these authors reported that the effect of the plot length on total runoff varied from negligible to significant for low erosivity events but it was limited for highly erosive events.

In any case, different calibration methods can be applied to obtain the experimental CN values. Moglen et al. (2022) compared alternative methodologies and they gave some practical suggestions on the most appropriate method to be used. Considering these suggestions of general validity requires supporting the results by Moglen et al. (2022) in other environments than those sampled by these authors.

Finally, the available scientific literature highlights that, for the method application at the plot scale, a research gap exists with reference to the expected scale effects on the experimental CN values, the description of the antecedent soil water conditions, and the assumptions concerning initial abstraction. An aspect that has not been investigated until now is the applicability of the method to plots subject to different erosive forms, that is, interrill and rill, since it is reasonable to expect differences due to different ways of runoff conveyance. Moreover, the calibration methods need to be compared for a given sampled site to identify which produces the best performance of the CN method.

Most of the investigations particularly focused on the USLE-MM and the USLE-MB have been carried out at the Sparacia experimental station of the Department of Agricultural, Food and Forest Sciences, Palermo University. It was established on clay soil and includes bare plots with lengths varying from 11 to 44 m and steepness values varying between 9% and 26%. Testing the CN method at this experimental station can help one step further in the direction outlined by Gao et al. (2012) of predicting event soil loss by coupling simple hydrological and soil erosion models.

The general objective of this investigation was first to establish the conditions, in terms of rainfall depth, type of erosion

process, and calibration approach, in which the NRCS-CN method (Equations 2 and 3) can be expected to perform better at Sparacia. Then, the possibility of coupling the simulated runoff and the USLE-MB (Equation 1) is assessed using data collected at the Sparacia station. The rainfall-runoff measurements performed during a prolonged observation period (2002–2019) were used to calibrate the CN at the plot scale. The specific objectives were to: (1) test the CN values from the National Engineering Handbook for Sparacia clay soil; (2) establish the specific initial abstraction ratio; (3) evaluate the CN variability; (4) investigate potential effects of plot slope, length, and antecedent soil moisture on CN; (5) test the reliability of the combination of the USLE-MB and CN method in predicting event soil loss.

2 | Materials and Methods

2.1 | Plot Description and Experimental Measurements

The Sparacia experimental station for soil erosion measurement is located in Sicily, South Italy, approximately 100 km south of Palermo. The climate is of Mediterranean semiarid type with an average annual rainfall of 700 mm. The soil is a Vertic Xerocept and has negligible gravel content. The 22 experimental plots installed at Sparacia (Figure 1) feature clay

soil (62% clay, 33% silt and 5% sand) and have different length l , width w , and steepness s . In detail, two plots of $22\text{ m} \times 2\text{ m}$ ($l \times w$) are characterised by $s = 9\%$, six plots of $22\text{ m} \times 8\text{ m}$ with $s = 14.9\%$ and a couple of replicated plots for each different size ($33\text{ m} \times 8\text{ m}$, $44\text{ m} \times 8\text{ m}$, $11\text{ m} \times 4\text{ m}$, $11\text{ m} \times 2\text{ m}$, and $22\text{ m} \times 2\text{ m}$) with $s = 14.9\%$ are established at the Sparacia station. A couple of $22\text{ m} \times 6\text{ m}$ plots with $s = 22\%$, and two plots of $22\text{ m} \times 6\text{ m}$ with $s = 26\%$ are also established in the experimental area. The oldest plots (four plots of $22\text{ m} \times 8\text{ m}$) were constructed in 1999 and the newest plots (9% sloped) in 2012. Due to the increasing extent of the experimental station over time, the number of available plot measurements varies with the *plot type*. In this paper, in accordance with the USLE scheme, a *plot type* identifies a combination of plot length l and steepness s , regardless of plot width. Indeed, with reference to the Sparacia station, Bagarello, Ferro, et al. (2011) demonstrated that plot width effects on event runoff varied from negligible to significant for low erosivity events and tended to vanish for highly erosive events, which are much more relevant as compared to the former in terms of modelling. The plots are maintained in cultivated fallow by tillage with a power cultivator in accordance with the reference condition of the USLE.

For each erosive event, rainfall intensity and total precipitation depth P (mm), runoff volume per unit plot surface Q (mm), and plot soil loss A_e (t ha^{-1}) were measured. The runoff coefficient Q_R was calculated as Q/P .

Rainfall intensity and total precipitation depth were recorded by two rain gauges located at two sites within the experimental area where the plots with $s = 9\%$ and 14.9% and those with $s = 22\%$ and 26% are installed, respectively. Runoff and sediments were collected into the tanks arranged in series downstream of each plot, varying in number from 1 to 3 as a function of the plot size. For example, the 11 m long plots are equipped with one tank, while the 44 m long plots are equipped with three tanks. The runoff Q was determined by the suspension level reading, as the geometric characteristics of the tanks are known. This is the net runoff volume, that is, excluding the volume occupied by the solid fraction, which is determined from its weight and the soil specific weight. The plot soil loss A_e was measured by sampling the suspension into the tanks or by direct weighing of all solid materials stored in the tanks. The latter method was used only when the sediment component sharply prevailed compared to the water component. In this case, the total weight of the stored suspension (liquid and solid fractions) in the tank was measured and a representative sample was extracted to determine the dry weight to wet weight ratio. The sampling of the suspension was applied otherwise, and A_e was obtained as the product of the suspension volume and the mean concentration measured by the sampling procedures described in other papers (Bagarello et al. 2004; Carollo et al. 2016; Pampalone et al. 2022) and in the Supporting Information S0.

The summary statistics for the 702 plot-event measurements of P and Q , performed from January 2002 to January 2019, are listed in Table 1. Within this monitoring period, soil moisture data were collected until May 2009. The gravimetric soil moisture was measured approximately every 2–3 weeks on three disturbed samples collected near the plots from both the top 0.05 m

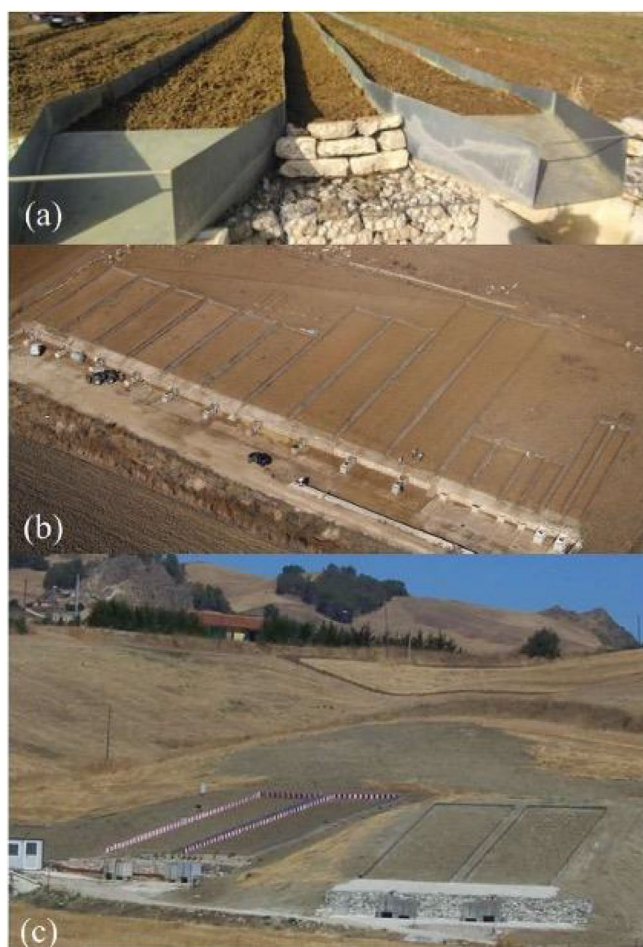


FIGURE 1 | View of the erosion plots with steepness s equal to (a) 9%, (b) 14.9% and (c) 22% and 26%.

TABLE 1 | Summary statistics of the measurements of total precipitation depth P , runoff Q and soil moisture θ .

	P (mm)	Q (mm)	θ (kg kg ⁻¹) ^a
Number of plot-event measurements for P and Q and number of measurements for θ	702	702	156
Min	11.8	0.03	0.05
Max	145.8	41.6	0.47
Mean	46.7	5.8	0.23
Median	41.6	4.0	0.22
CV	0.61	1.01	0.54

^aMonitoring period limited to 2002–2009.

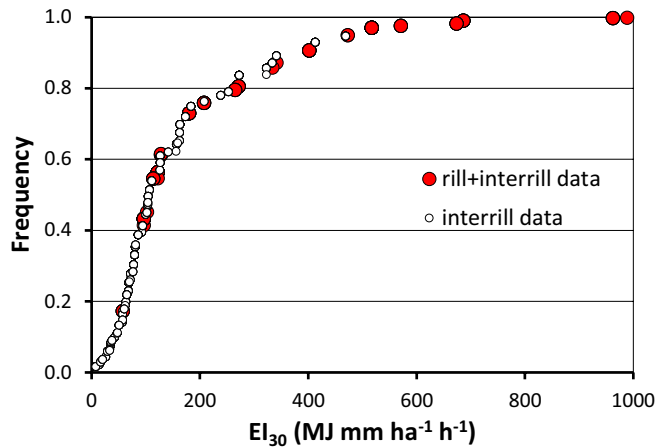


FIGURE 2 | Cumulative frequency distribution of the rainfall erosivity index EI_{30} for events with different erosive forms.

of soil and the 0.05–0.10 m layer and oven-dried. The total number of sampling dates was equal to 122. The three measured values for each layer were averaged for each sampling date to obtain the mean soil moisture, θ (kg kg⁻¹). As reported in the results section, the soil moisture θ from the top 0.05 m of soil was used in the present analysis. The 122 measured values varied from 0.05 to 0.47 kg kg⁻¹ (Table 1).

Depending on the erosive event, plots experienced only interrill erosion or interrill and rill erosion simultaneously, with the former occurring much more frequently than the latter. Figure 2 shows that events with rill formation fall in the upper tail of the cumulative frequency distribution of EI_{30} . Moreover, half of the EI_{30} measurements for events with rill formation have a not-exceeding frequency $\geq 80\%$, confirming that rills originated from the higher erosive rainfall events. Rills were always obliterated by tillage to restore identical plot surface conditions before the following erosive event. The datasets considered in this investigation refer to all available data (AD), data recorded for erosive events in which only the interrill component was detected (ID), and data deriving from both interrill and rill erosion (RD). In the latter case, rill channels were visually appreciable in the plot surface, and the rill component significantly contributed to total soil loss.

2.2 | Testing the CN Values From the National Engineering Handbook

Initially, the CN values from the National Engineering Handbook (NEH) (NRCS 2004a, 2004b) were tested with the available measurements. As these values neglect possible slope effects, the standard CNs were also slope-adjusted using the following Sharpley and Williams's (1990) equation:

$$CN_{II,s} = a(CN_{III} - CN_{II})(1 - be^{-cs}) + CN_{II} \quad (4)$$

where a , b and c are three coefficients equal to 0.333, 2 and 13.86, respectively, and s is the slope expressed as $m m^{-1}$. Also, CN_{II} and CN_{III} are CN values for average Antecedent Moisture Condition (AMC II) and AMC III (wet), respectively, and $CN_{II,s}$ is the adjusted CN_{II} that is assumed to apply for $s = 0.05$.

2.3 | Determination of the Initial Abstraction Ratio and CN Calibration

For each of the seven plot types ($l = 22$ m, $s = 9\%$; $l = 11$ m, $s = 14.9\%$; $l = 22$ m, $s = 14.9\%$; $l = 33$ m, $s = 14.9\%$; $l = 44$ m, $s = 14.9\%$; $l = 22$ m, $s = 22\%$; $l = 22$ m, $s = 26\%$) the calibration was performed for 18 combinations (from C1 to C9 for each calibration approach, Table 2) of three rainfall ranges (full set of P , events with P under the median value of 41.6 mm, events with P exceeding the median value), two calibration approaches (median value, MV, and least-squares, LS, as defined below) and three datasets (AD, ID, RD). Table 2 shows the acronyms that identify all the combinations and the related sample size N including all plot types, which varies from 43 to 702.

Following Moglen et al. (2022), the median value (MV) and the least squares (LS) approaches were applied for CN calibration.

For each rainfall-runoff (P , Q) observation, the following S value that satisfies Equation (2) is determined:

$$S = \frac{2\lambda P - \lambda Q + Q - \sqrt{\lambda^2 Q^2 - 2\lambda Q^2 + 4\lambda PQ + Q^2}}{2\lambda^2} \quad (5)$$

Introducing Equation (5) into Equation (3), the individual experimental CN value, corresponding to each pair (P , Q), is determined.

With the MV approach (Mishra et al. 2007), the median of these CN values was set as the calibrated CN and applied to calculate plot runoff. With the LS approach, the calibrated S value was calculated by applying the least-squares technique to minimise the following objective function Z :

$$Z = \sum_{i=1}^N (Q_i - Q_{\text{calculated},i})^2 \quad (6)$$

where Q_i and $Q_{\text{calculated},i}$ are the measured runoff value and that calculated by Equation (2) for the single rainfall event, respectively. The calibrated S value was then converted into the calibrated CN for a given plot type by Equation (3). The pattern of the calibrated CN against plot length and steepness was also analysed.

TABLE 2 | Acronyms identifying the combinations of the three rainfall ranges, two calibration approaches (MV and LS) and three datasets (AD, ID, RD) used in this investigation with the related sample size N including all plot types.

	MV			LS		
	$11.8 \leq P \leq 145.8$	$11.8 \leq P \leq 41.6$	$41.6 < P \leq 145.8$	$11.8 \leq P \leq 145.8$	$11.8 \leq P \leq 41.6$	$41.6 < P \leq 145.8$
AD	C1-MV	C4-MV	C7-MV	C1-LS	C4-LS	C7-LS
N	702	369	353	702	369	353
ID	C2-MV	C5-MV	C8-MV	C2-LS	C5-LS	C8-LS
N	587	297	310	587	297	310
RD	C3-MV	C6-MV	C9-MV	C3-LS	C6-LS	C9-LS
N	115	72	43	115	72	43

Abbreviations: AD = all data; ID = interrill data; LS = least squares calibration approach; MV = median value calibration approach; P = rainfall depth in mm; RD = rill + interrill data.

The CN calibration needs the preliminary determination of the appropriate value of the initial abstraction ratio λ , which was carried out using all the available experimental information (702 data). Different λ values, falling within the range derived from literature ($\lambda \leq 0.2$), were applied and, for each of them, the calibrated CN for a given plot type was obtained by Equations (3) and (5) and the MV approach described above. Considering that all the rainfall events used here produced runoff, the compliance of the condition $P - \lambda S > 0$ was imposed in determining λ . In addition, to assure the better quality of runoff estimations, λ was optimised by minimising the relative standard error RSE, defined below, calculated on the 702 data. In other words, the λ value was determined as that value simultaneously ensuring the absence of null runoff predictions and minimisation of RSE.

2.4 | Relation Between the Individual Experimental CN Values and Hydrological Variables

An attempt to explain the expected CN variability for a given plot type was performed by relating experimental CNs to soil moisture before the erosion event. Specifically, the θ values from the top 0.05 m of soil and measured within an interval of i days ($i = 1, 2, 3, 4, 5$) before the erosion event were considered as (i) soil moisture in the top layer (0–0.05 m) was better related to CN as compared to that in the 0.05–0.10 m and 0–0.10 m layers, and (ii) the related measurement should have been performed shortly before the erosion event to be effectively related to runoff. For best exploiting all the available experimental information, the effect of soil moisture on CN was explored starting from the 702 CN values from the C1-MV. However, considering the actual availability of the θ measurement shortly before the erosion event, the number of θ –CN pairs ranges from 52 (1-day antecedent soil moisture) to 139 (θ measured within the 5 days—interval before the event).

For the largest data series ($l = 22$ m, $s = 0.149$) a multiple log-linear regression of the experimentally determined CN against θ and P was performed, while the regression analysis was not

carried out for other plot types because of the limited sample sizes.

2.5 | Soil Loss Estimations by USLE-MB

As demonstrated in the result section, the CN method was reliable in predicting runoff only for rill events. Therefore, Equation (1), with the simulated Q_R value, was applied to estimate soil loss, A_e , for these events. In particular, the soil loss data set was split into events with a rainfall depth P lower than or equal to 41.6 mm and events with $P > 41.6$ mm to be consistent with the previous runoff analysis. In other words, data belonging to C6-LS and C9-LS combinations (Table 2) were used, whose corresponding CN values are reported on S6 and S9 in the Supporting Information. For each rainfall range and plot type, the runoff depth estimated with the LS approach was divided by the rainfall depth to estimate the runoff coefficient Q_R .

A workflow summarising all the steps from the Section 2.2 to the Section 2.5 is reported in Figure 3.

2.6 | Performance Evaluation

The RSE was applied to quantify the quality of the runoff estimations with both MV and LS approaches (Moglen et al. 2022), and the soil loss estimations by the USLE-MB (Equation 1):

$$RSE = \frac{Z^{0.5}}{\sigma(N-2)^{0.5}} \quad (7)$$

in which σ is the standard deviation of the measured runoff values. The modelled runoff and soil loss values are better than the mean of the measurements if $RSE < 1$. A single RSE value was determined for (i) each plot type within each combination, and (ii) each combination regardless of plot type (Supporting Information from S1 to S9) which synthesises the overall CN performance.

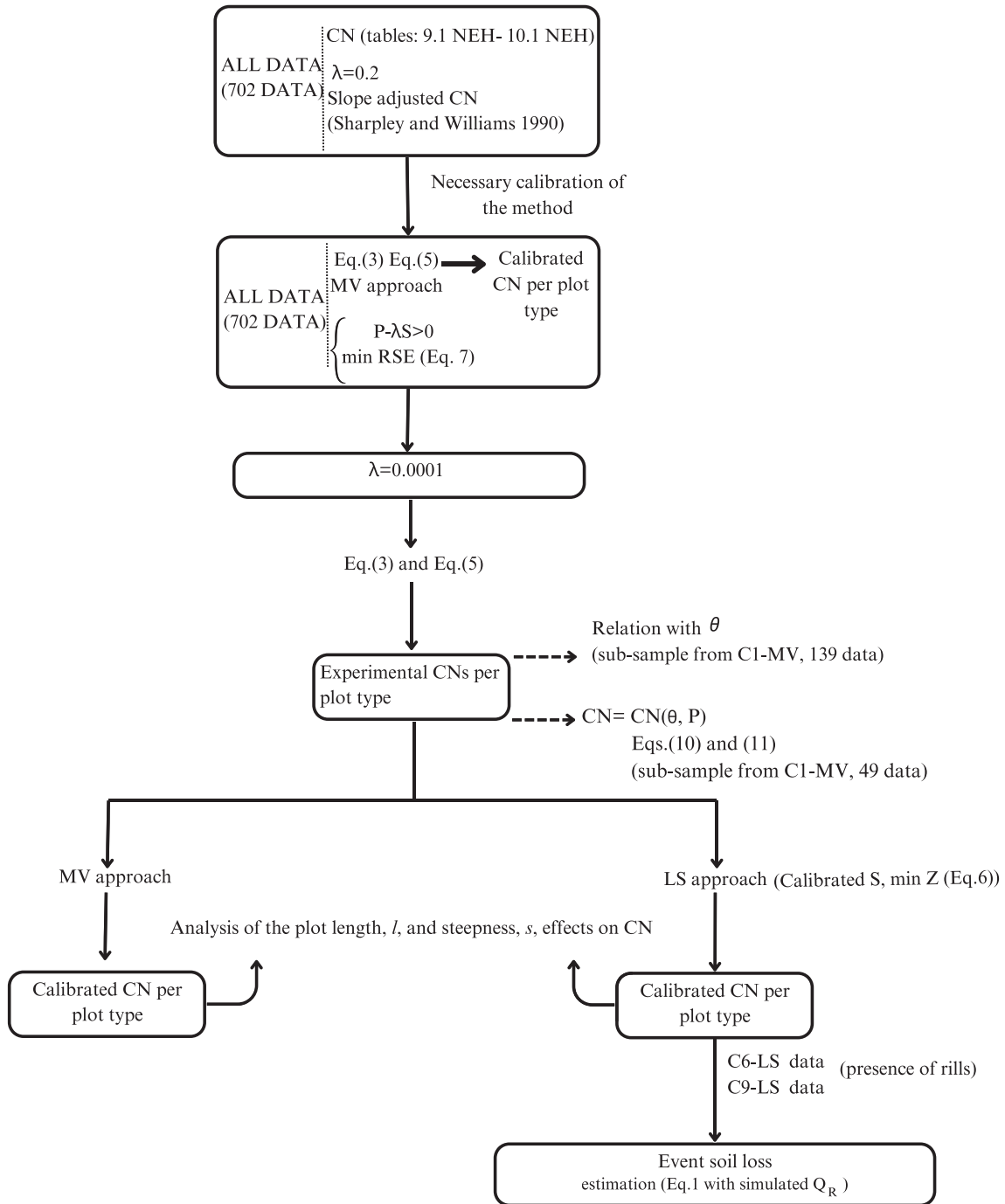


FIGURE 3 | Flowchart concerning the methods applied in this investigation.

The Nash and Sutcliffe efficiency index (Nash and Sutcliffe 1970), NSEI, expresses the relative magnitude of the residual variance compared with the measured data variance, and is related to the RSE through the following relationship:

$$NSEI = 1 - \frac{(N - 2)}{(N - 1)} RSE^2 \quad (8)$$

When the model accounts for all the variation in the measurements, NSEI = 1, while NSEI = 0 and NSEI < 0 indicate that the model predictions are as accurate as the mean of the measurements and worse than the measured mean, respectively. In this paper, this index was used for comparison purposes with

literature studies (Huang et al. 2006, 2007; Fu et al. 2011; Lal et al. 2015; Shi et al. 2018).

In addition to the relative standard error (Equation 7), the frequency distribution of the absolute value of the normalised runoff prediction error, $|Er|$, was determined for the combination for which the runoff model performed best. $|Er|$ (%) is calculated for each data pair of measured, Q , and calculated, $Q_{\text{calculated}}$, runoff depth as:

$$|Er| = 100 \left| \frac{(Q - Q_{\text{calculated}})}{Q} \right| \quad (9)$$

3 | Results

3.1 | Testing the CN Values From the National Engineering Handbook

According to the criteria reported on tab. 7.1 of the National Engineering Handbook (NEH) (NRCS 2009), the Sparacia clay soil is assigned to the D hydrologic soil group. For the investigated bare soil and $\lambda=0.2$, the CN from the NEH tab. 9.1 (NRCS 2004b) is equal to 94, for an average Antecedent Runoff Condition (ARC II). Currently, ARC comprehensively represents the causes of CN variability (rainfall intensity and duration, total rainfall, soil moisture conditions, cover density, stage of growth, and temperature) and is in place of the AMC that was considered in previous NEH versions and focused on the antecedent soil moisture.

For dry (ARC I) and wetter (ARC III) conditions, CN is equal to 85 and 98, respectively (tab. 10.1 of NEH; NRCS 2004a). Figure 4 shows that the individual CN values for any ARC overestimate runoff for more than 80% of data. In addition, the poor performance is demonstrated by very high RSE values ranging from 4.2 to 7.6. The application of the Sharpley and Williams's (1990) equation (Equation 4) produced more marked runoff overestimations and worsened the method performance ($4.3 \leq RSE \leq 32.5$).

3.2 | Initial Abstraction Ratio λ

Figure 5 shows, for discrete values of the initial abstraction ratio falling within the range of literature values ($\lambda \leq 0.2$), the number n of null predictions (Figure 5a) and RSE values (Figure 5b) against λ , respectively. For $\lambda < 0.03$, all the runoff predictions differ from 0, while n increases rapidly as λ increases in the range 0.03–0.2. The relative standard error decreases as λ decreases to 0.0001, while it is almost constant and equal to 1.38 under this λ value. Considering these results, the optimised abstraction ratio was set to 0.0001. In any case, the high value of the minimum RSE underlines the inadequacy, for the complete dataset (C1-MV combination), of using a specific CN for plot type (l, s), which contrasts with the original approach developed to be applied at the watershed scale. Therefore, attempts are made in the following to investigate potential effects due to plot slope and length, soil moisture before an erosive rainfall event, and rainfall depth.

3.3 | CN Variability

For the 18 investigated combinations (Ci-MV and Ci-LS combinations, with $i=1$ to 9), Figure 6 shows the ranges of CN, that is, the domains of the values calibrated for the seven plot types, and the RSE values determined for N runoff predictions of each combination using the specific CNs per plot type. Overall, the CN varies greatly from 4.6 to 78 while RSE is from 0.64 to 1.38.

Concerning the entire (Figure 6a,b) and interrill (Figure 6c,d) datasets, the 11.8–41.6 mm rainfall range produces wider CN ranges and with higher maxima as compared to the other two rainfall ranges, regardless of the calibration method. The

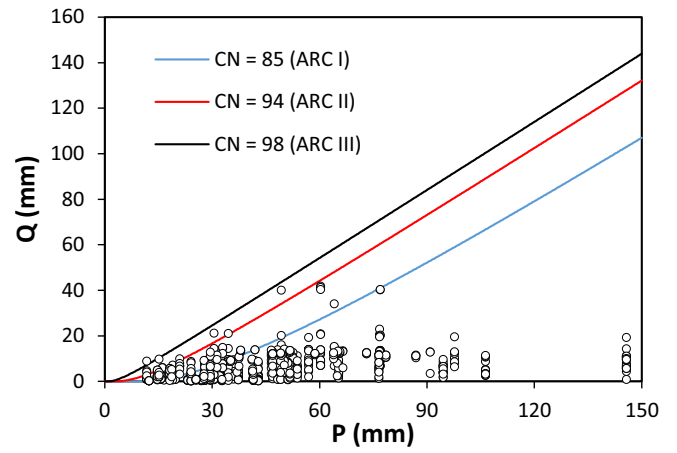


FIGURE 4 | Comparison between the rainfall depth P –runoff Q experimental pairs and the curves representing the modelled runoff values with CNs from the National Engineering Handbook and different Antecedent Runoff Conditions (ARCs).

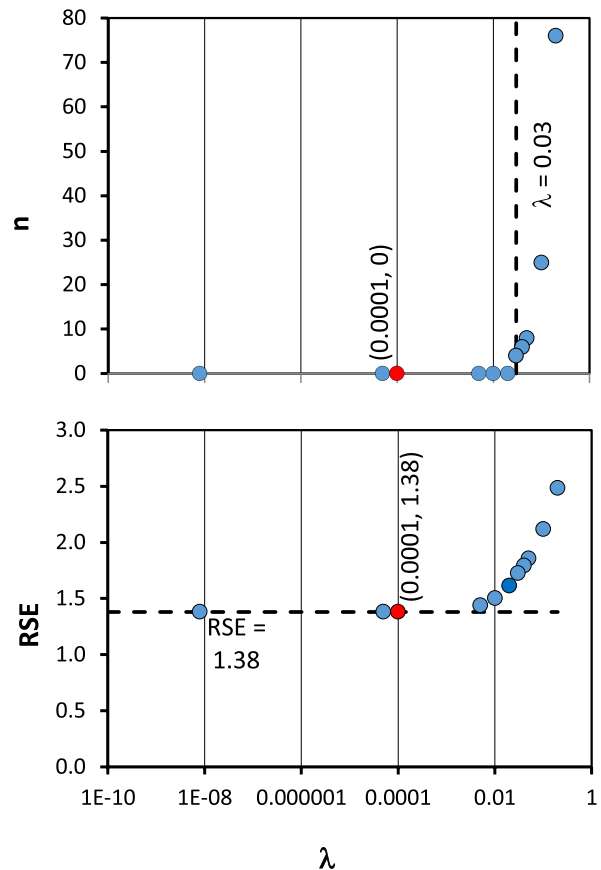


FIGURE 5 | Plot of the number of null runoff predictions, n , and the relative standard error, RSE, against the initial abstraction ratio, λ , for the C1-MV combination.

minimum values mirror the same behaviour as the maxima for the LS approach while they are substantially independent of the rainfall range for the MV approach. For the rill dataset (Figures 6e,f) and both the calibration approaches, the extent

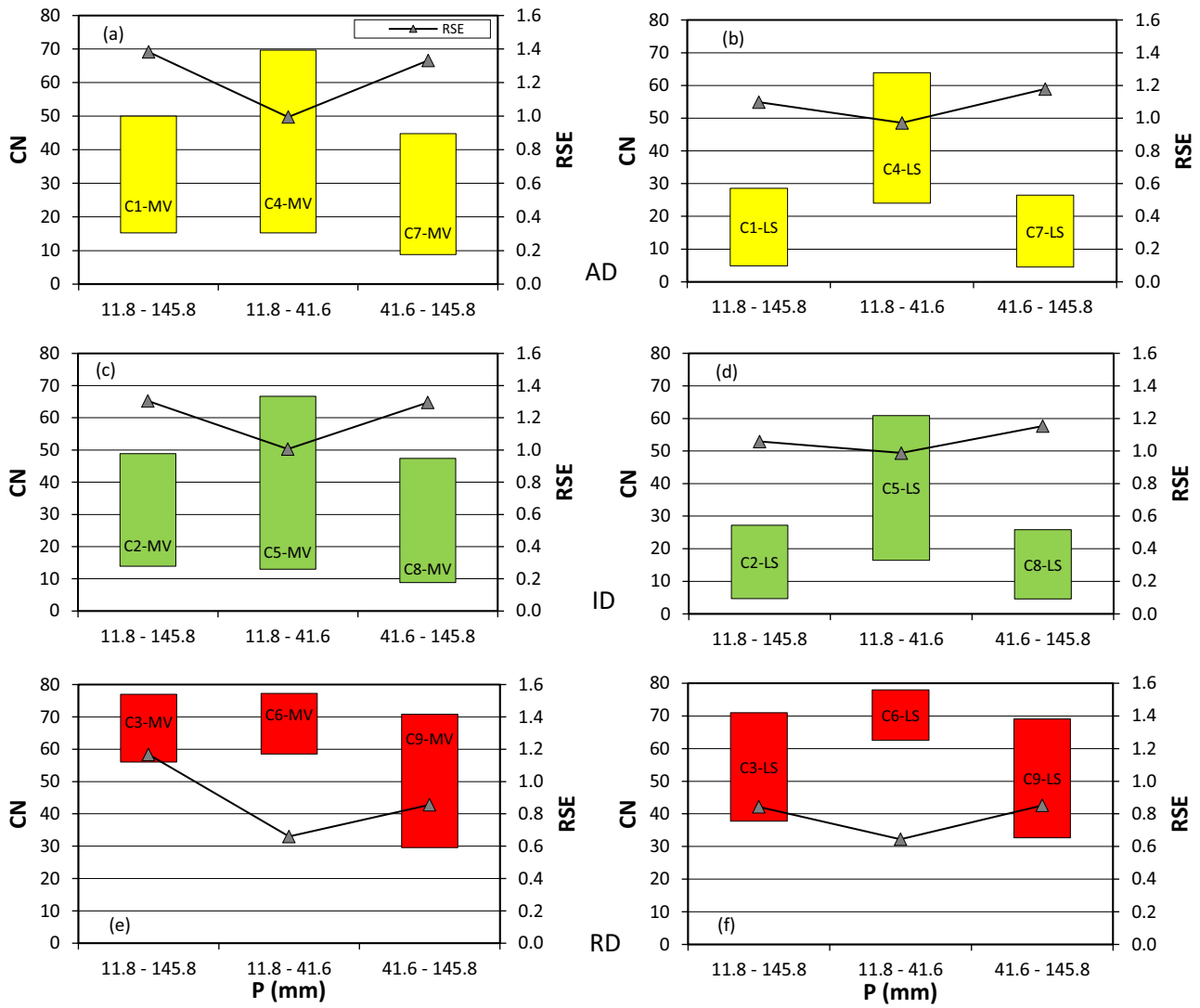


FIGURE 6 | Ranges of the calibrated CN and values of RSE for AD (a, b), ID (c, d) and RD (e, f) and the 18 examined combinations reported in Table 2.

of the CN range fluctuates among the three considered rainfall depth ranges (11.8–145.8 to 11.8–41.6 and 41.6–145.8 mm). The maxima are comparable across the rainfall ranges and the minimum values for P over the median (MV approach) or under the median (LS approach) differ significantly from the ones obtained for the other two rainfall intervals.

For fixed rainfall range, similar CN intervals are obtained for AD and ID, while higher CNs feature RD, regardless of the calibration approach.

3.4 | Best Combination of Rainfall Range, Applied Dataset and Calibration Approach to Estimate CN

The reliability of the CN model depends on the dataset, as demonstrated through the relative standard errors of Figure 6. The quality of the runoff estimates is comparable ($RSE \approx 1$) or worse ($RSE > 1$) than the mean of the measurements for AD

and ID, while it is generally better than the mean ($RSE < 1$) for RD. In any case, the LS approach allows for better runoff estimates than the MV approach and the RSE minimum value (0.64–0.66) is detected for the 11.8–41.6 mm rainfall range. Finally, the model is useful to predict plot runoff when rill channels develop during the erosion events and works the best when it is calibrated with the LS approach and events with rainfall depth under the median value recorded over the monitoring period.

3.5 | Effects of Plot Length, Steepness and Soil Moisture on CN

To check for plot length and steepness effects on runoff, as stated above, the calibration was performed for individual plot types. Figure 7 illustrates, as an example concerning the C4-MV and C4-LS combinations, the experimental and calibrated CNs arranged for plot length (Figure 7a) and steepness

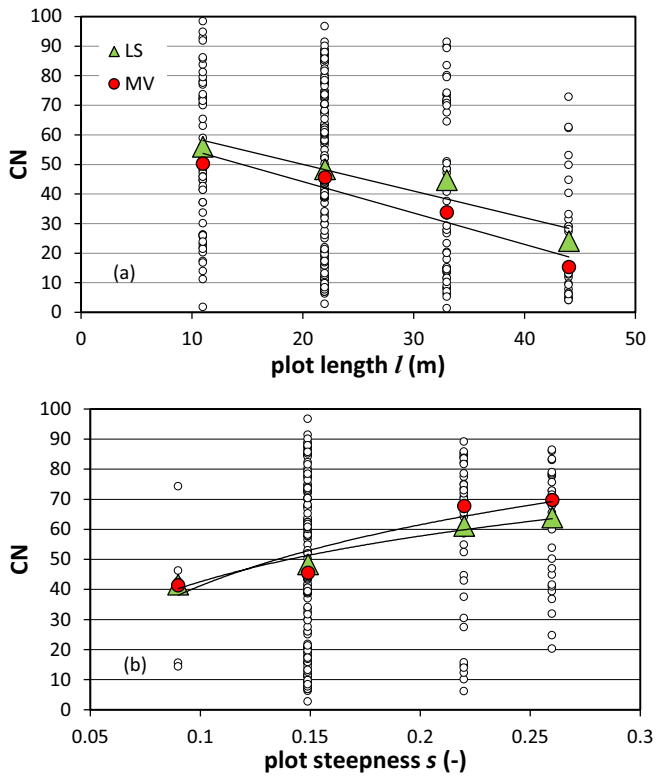


FIGURE 7 | Relationship between the CN values calibrated with the mean value (MV) and least squares (LS) approaches and (a) plot length and (b) plot steepness for C4-MV and C4-LS. White dots indicate the experimentally determined CN values. The regression equations refer to the calibrated CNs.

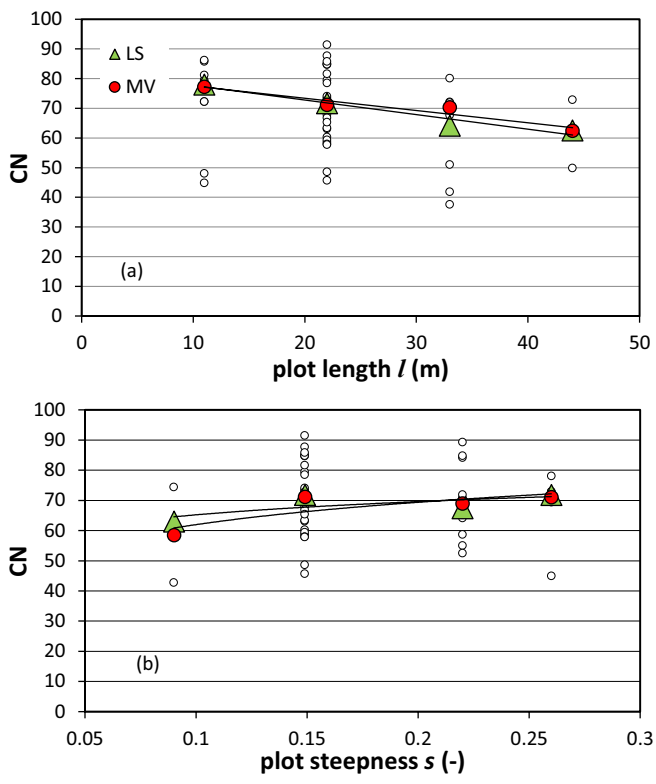


FIGURE 8 | Relationship between the CN values calibrated with the mean value (MV) and least squares (LS) approaches and (a) plot length and (b) plot steepness for C6-MV and C6-LS.

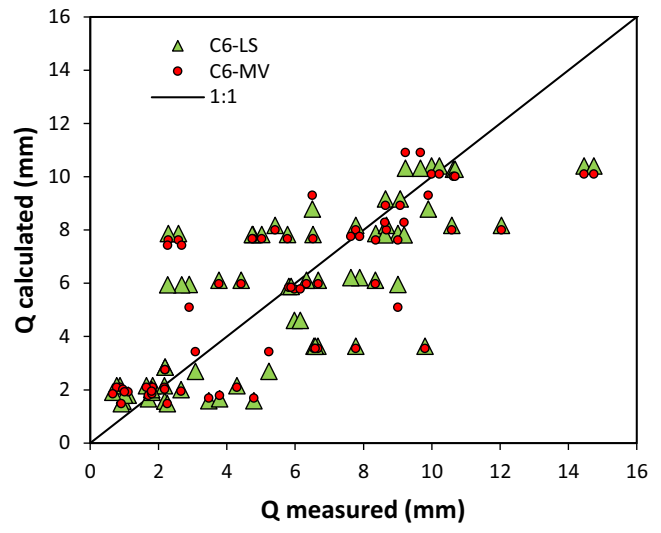


FIGURE 9 | Comparison between the measured and calculated runoff values for C6-MV and C6-LS.

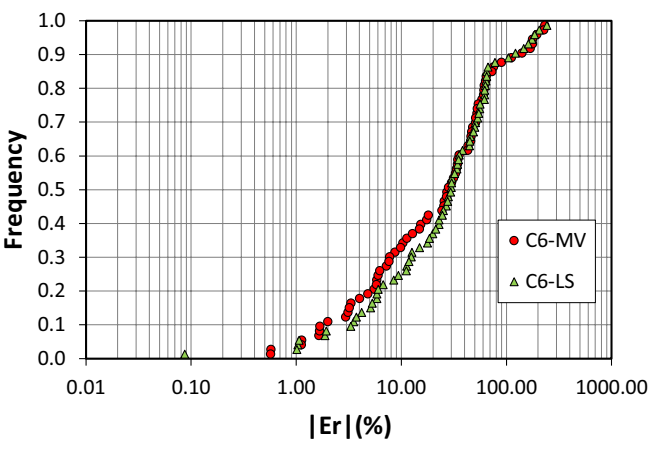


FIGURE 10 | Cumulative frequency distributions of the absolute value of the normalised runoff prediction error, $|Er|$ for C6MV and C6LS.

(Figure 7b). Again, a high CN variability is apparent but CN decreases for increasing l values and increases with s . There are negligible to moderate differences in the calibrated CN values between calibration approaches. Similarly, Figure 8 shows results for the C6-MV and C6-LS combinations, for which the runoff model works best. For each plot type, the CN variability is high but reduced as compared to the former case, and the inverse relation between CN and plot length is confirmed while the direct relationship of CN against plot steepness is confirmed but weakened. Negligible differences in the calibrated CN values exist between MV and LS approaches, and the predicted runoff values reproduce the measured ones in an only approximately satisfactory manner (Figure 9) as absolute errors $|Er|$ are less than 50% for 69% of the predictions but they are extremely high for 11% of them (Figure 10). The NSEI is equal to 0.59.

The above trends of CN with plot length and steepness were always detected except for 3 out of 36 cases (3 rainfall ranges \times 3 datasets \times 2 calibration approaches \times 2 relationships) (see S3 and

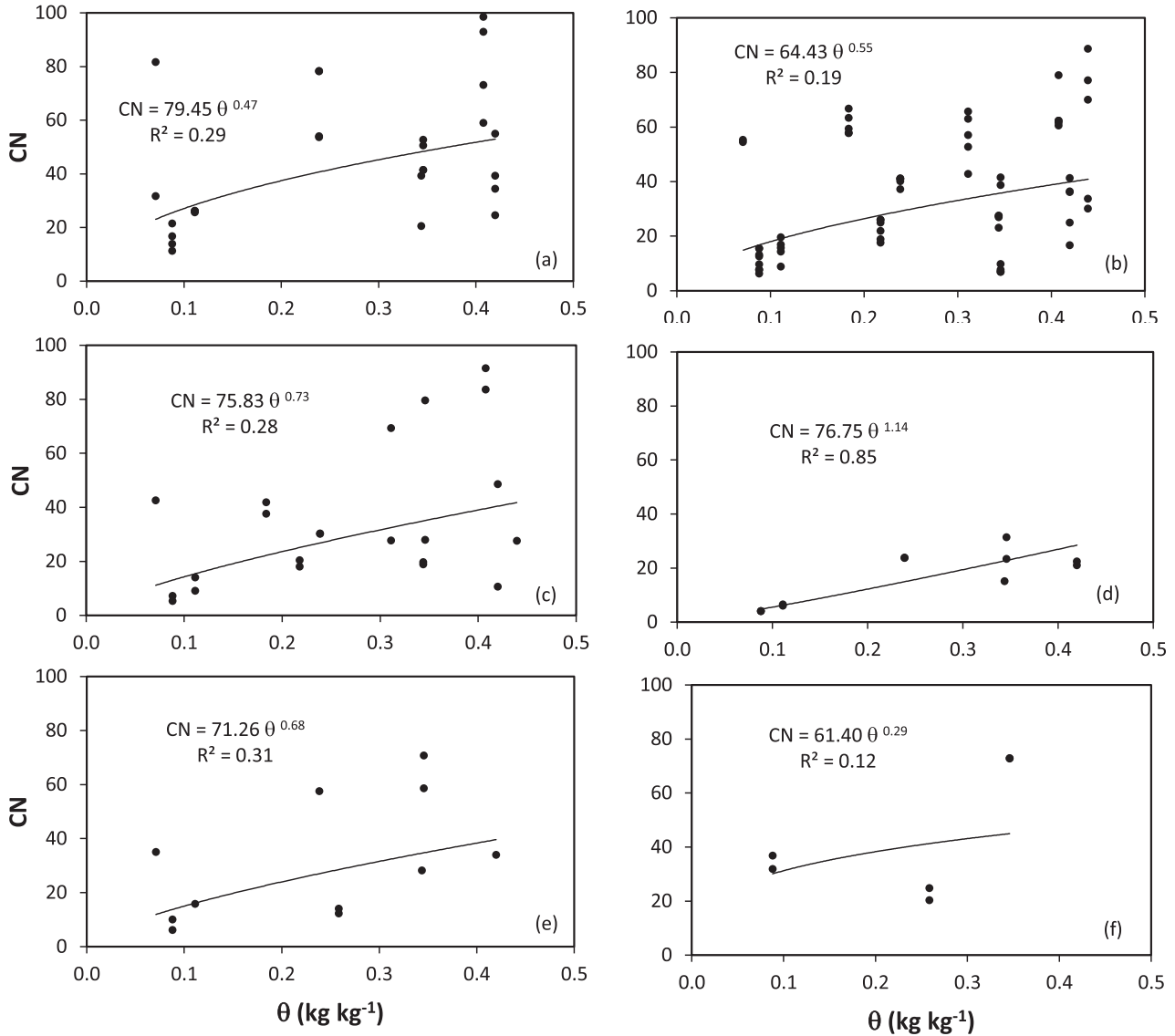


FIGURE 11 | Plot of the experimental CN values against the gravimetric soil moisture θ for plots with (a) $l=11$ m and $s=14.9\%$, (b) $l=22$ m and $s=14.9\%$, (c) $l=33$ m and $s=14.9\%$, (d) $l=44$ m and $s=14.9\%$, (e) $l=22$ m and $s=22\%$ and (f) $l=22$ m and $s=26\%$.

S9, Supporting Information), all referred to the CN vs. s relation and the C3-LS, C9-MV and C9-LS combinations. An acceptable to good agreement between the CN values calibrated with MV and LS approaches was found for 6 out of 9 comparisons (from S4 to S9, Supporting Information).

To assess the variability of the experimental CN for given plot type, Figure 11 shows the 139 θ -CN pairs arranged for plot type, with θ measured within the 5 days-interval before the event. The only not represented plot type is that with $s=9\%$ because there are no available soil moisture measurements. The general result is that, as expected, CN tendentially increases with soil moisture, but the points are greatly scattered around the best fit power relationships. This result is also representative of those obtained with θ measured within the time intervals of 1 to 4 days before the event. Figure 11 shows that the coefficient of determination R^2 related to these relationships ranges from 0.12 to 0.31 with a single exception of 0.85 and is equal to 0.19 for the largest data

series ($l=22$ m, $s=0.149$, 61 data). For the latter, the multiple log-linear regression of the experimentally determined CN against θ and P resulted in:

$$CN = 79.20 \theta^{0.542} P^{-0.062} \quad (10)$$

which is characterised by $R^2=0.195$. A significant relative increase of R^2 from 0.195 to 0.41 was observed for the following Equation (11):

$$CN = 119.35 \theta^{0.740} P^{-0.153} \quad (11)$$

which is based on the sample restricted to rainfall-runoff events without rills (49 data), but the estimated performance remains poor (Figure 12). This sub-sample was selected as it allows for the specification of the erosive form, in addition to plot size and steepness, maintaining simultaneously a sufficient sample size to perform the regression analysis.

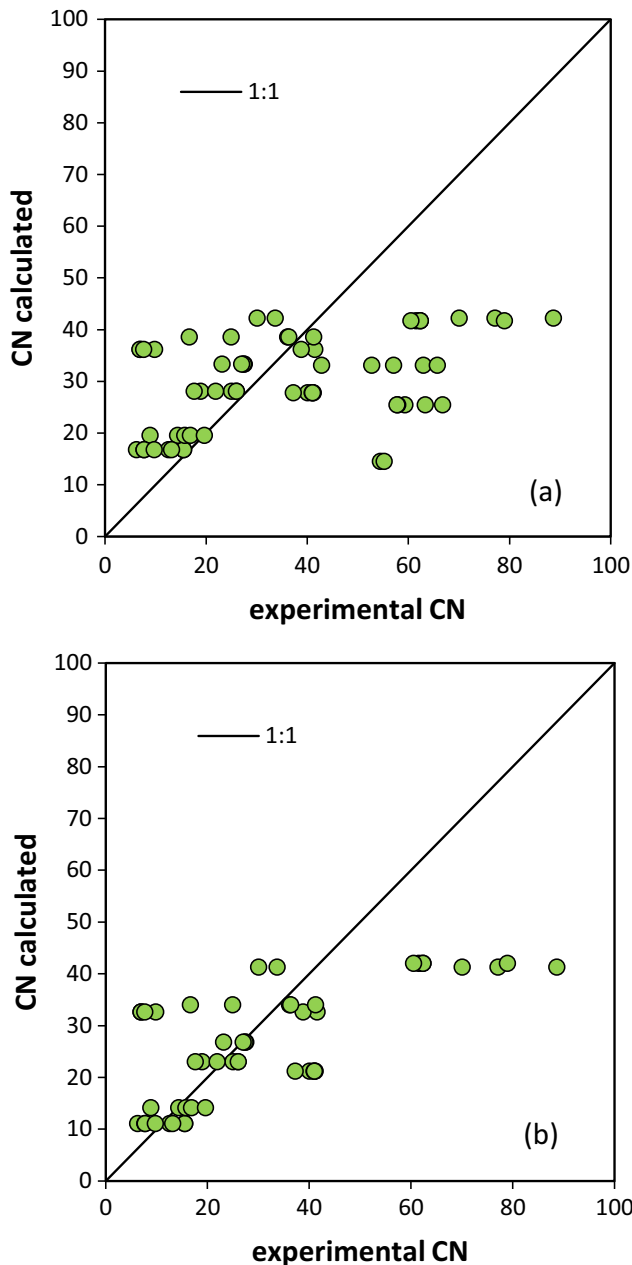


FIGURE 12 | Comparison between the experimental values of CN, obtained by Equations (3) and (5), and those calculated by (a) Equation (10) and (b) Equation (11).

3.6 | Coupling USLE-MB Model With Simulated Runoff by CN Method

The benchmark for the performance assessment of the USLE-MB with the simulated runoff is the USLE-MB with the measured runoff. For comparison purposes, Figure 13 shows the scatterplots of the measured A_e values against the A_e values estimated by the USLE-MB (Equation 1) with the simulated (Figure 13a,c) and measured Q_R (Figure 13b,d), distinguished for rainfall range. The scatter of the data points around the line of perfect agreement reduces from the lower to the upper rainfall range, regardless of the applied runoff coefficient. For $11.8 \leq P \leq 41.6$ mm, RSE is equal to 1.04 (NSEI = -0.06) and

0.96 (NSEI = 0.09) in the case of simulated and measured runoff, respectively. For $41.6 < P \leq 145.8$ mm, RSE is equal to 0.69 (NSEI = 0.54) for the simulated runoff and 0.48 (NSEI = 0.77) for the measured runoff.

Figure 14 compares the soil loss values estimated by Equation (1) using the simulated and measured Q_R . The scattering of the data points for $11.8 \leq P \leq 41.6$ mm reflects that depicted in Figure 9 for runoff as soil loss is proportional to a power of the runoff coefficient according to USLE-MB (Equation 1) and is similar to the scattering of estimated soil loss values for $41.6 < P \leq 145.8$ mm.

4 | Discussion

4.1 | Testing the CN Values From the National Engineering Handbook

The results indicate extremely poor runoff estimates by the standard CN values for any ARC that cannot represent the event hydrologic response of the sampled plots. This expected result is due to the nature of the model that ignores factors influencing the rainfall-runoff transformation process, such as spatial scale effects or rainfall depth. Indeed, Figure 4 shows a runoff variability for a given rainfall depth that the model cannot reproduce because it has a single numerical parameter.

The Sharpley and Williams's (1990) equation assumes that the standard CN corresponds to a slope of 5% and gives a slope-adjusted CN that increases for increasing slope. Considering that the slope of the investigated plots varies from 9% to 26%, the use of these slope-adjusted CN values produced more marked runoff overestimations and worsened the method performance.

The standard model almost systematically overestimated runoff from the sampled bare plots, while contrasting results were obtained by Huang et al. (2006, 2007) and Gao et al. (2012). Huang et al. (2006) tested the model using plots with a vegetation cover of pasture ($s = 17\% - 140\%$) and alfalfa ($s = 14\% - 18\%$), while Huang et al. (2007) used plots with millet ($s = 40.4\% - 46.7\%$), pasture ($s = 57.7\%$), and potato cover. The plots related to the study by Gao et al. (2012) were covered with sparse apricot, dense shrubs with an arborous layer, and dense tussock and beard grass, respectively, while the slope steepness ranged from 34% to 47%. In all three investigations, plots had comparable sizes to the Sparacia ones. Huang et al. (2006) found that the standard CN method underestimated large runoff events (> 5 mm) but overestimated some of the small runoff events. According to Huang et al. (2007) the standard CN method generally underestimated runoff events, while for Gao et al. (2012) it significantly underestimated the observed runoff. Finally, the standard model application produces inaccurate runoff estimates for both bare plots and plots with vegetation cover, but with estimate errors having opposite signs.

4.2 | Initial Abstraction Ratio λ

By definition, the initial abstraction ratio λ of Equation (2) depends on soil and cover characteristics and increases when favourable conditions for interception, infiltration and surface

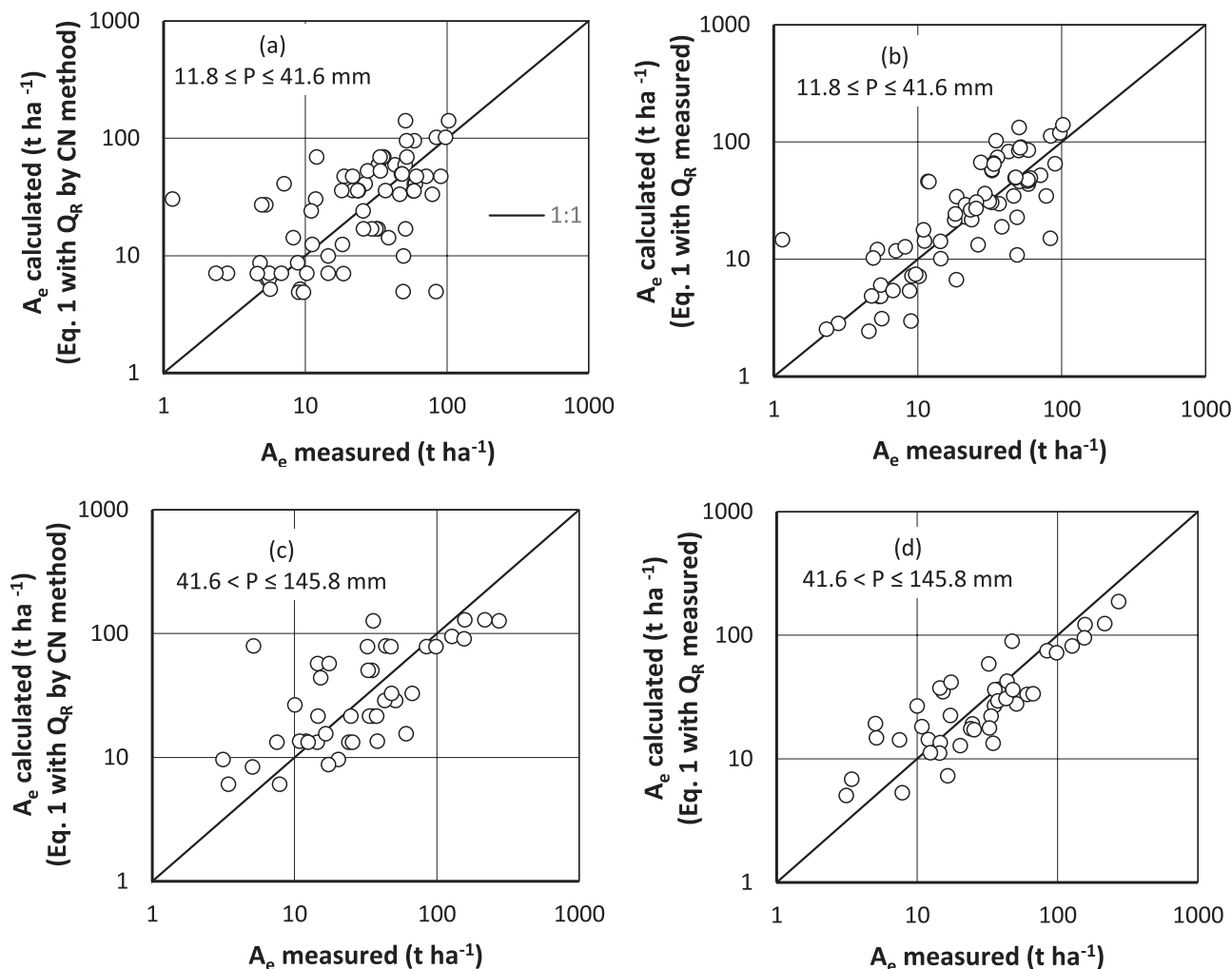


FIGURE 13 | Comparison between the measured soil losses, A_e measured, and those calculated by Equation (1) and (a) the CN method for the lower rainfall range, (c) the CN method for the upper rainfall range, (b) the measured runoff coefficient for the lower rainfall range, (d) the measured runoff coefficient for the upper rainfall range.

storage before runoff formation occur. The experimentally determined low value (0.0001) (Figure 5) is determined by the coexistence of three different factors that reduce λ . They are the absence of vegetation cover, the low-prone soil to infiltration, and the circumstance that the plot surface is a rough inclined plane without significant depressions. The selected λ value is much less than the long-standing value of 0.2 or that of 0.05 (Hawkins et al. 2009; Lal et al. 2017) suggested in recent literature, but it is in line with those obtained in some cases by different authors (Hawkins et al. 2002; Huang et al. 2007; Lal et al. 2015) by calibrating the CN method at plot scale.

4.3 | CN Variability and Best Combination of Rainfall Range, Applied Dataset and Calibration Approach to Estimate CN

For both calibration approaches, the analysis of Figure 6 demonstrates that the calibrated CNs for rainfall events with total precipitation depth higher than the median were generally slightly smaller than those calibrated on the entire dataset. The RSE

values corresponding to the former case were substantially like those obtained for the latter case except for the C3-MV and C9-MV combinations (Figure 6e). The calibrated CNs for rainfall events with total precipitation depth less than the median were generally higher than those calibrated on the entire dataset and gave improved model performances (smaller RSE), especially for the MV approach. In other words, the threshold of the median rainfall was only effective with reference to low and moderate rainfalls.

The comparable sample size between AD and ID explains the agreement in terms of CN range and quality of runoff estimates, while the higher CN values for RD capture the increased capability for runoff conveyance and accumulation when rill channels incise plots (Figure 6). Typically, the generation of a rill network promotes efficient runoff transport from hillslopes as rill channels concentrate runoff, thus increasing flow velocity and reducing the probability of water infiltration.

Results showed that the median value and the least-squares calibration approaches were indifferently applicable for most of the

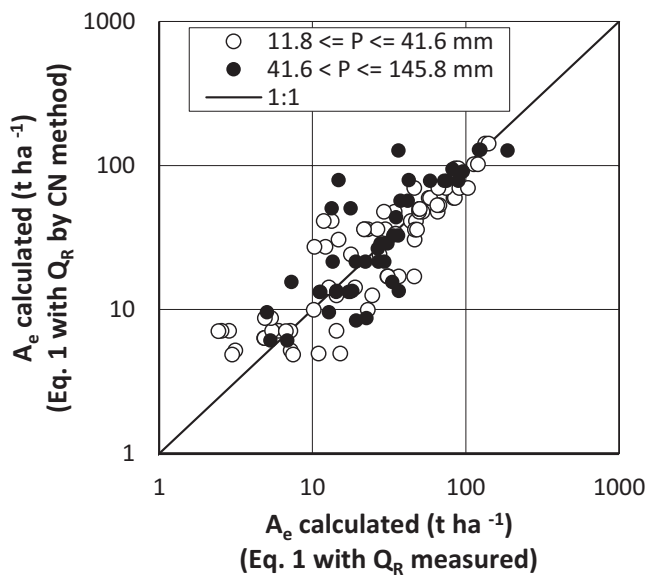


FIGURE 14 | Comparison between the soil loss values, A_e , calculated by Equation (1) with the measured runoff coefficient Q_R and by Equation (1) with Q_R estimated through the CN method, under two different rainfall ranges.

addressed cases, for which they provided similar CN and RSE values. However, in accordance with Moglen et al. (2022), the LS approach was preferable since it yielded smaller RSE values than the MV ones.

The advantage of using the CN method to model, even though in an approximately satisfactory manner (Figures 9 and 10), plot runoff at the Sparacia area is limited to the events with rill formation, which are usually characterised by a relevant climatic forcing (Figure 2) and more runoff compared to interrill events. Although they are not dominant in the current database, it is widely recognised and even observed at Sparacia that a great amount of yearly or long-term soil loss is due to a few relevant erosion events (e.g., González-Hidalgo et al. 2007; Bagarello et al. 2017), in which rill formation is likely to occur. Therefore, modelling runoff for predicting soil loss by USLE-M, USLE-MM, and USLE-MB is particularly important for these events, and the CN method appears to be suitable. The maximum NSEI value of 0.59, obtained for C6-MV and C6-LS, is higher than the values (0.25–0.51) obtained by Fu et al. (2011) in two experimental stations. In addition, the results of these authors indicated a decreasing number of acceptable predictions under different ranges of rainfall depth, that is in the passage from $P \leq 25$ mm to $25 < P \leq 50$ mm and $50 < P \leq 100$ mm. This finding qualitatively agrees with that detected here concerning better runoff estimations under P less than the median value (41.6 mm) compared to $P > 41.6$ mm. The NSEI is also slightly higher than that obtained by Lal et al. (2015) with an optimised Sharpley and Williams's (1990) equation. It is worth noting that they also obtained NSEI values of 0.702 to 0.796 for runoff estimations by regression models of CN vs. 1-day antecedent soil moisture and 5-day antecedent rainfall, respectively, but the reported performance statistics are limited to 3 plots out of 24. For the data from the pasture and alfalfa plots by Huang et al. (2006) in the steep slopes of Loess Plateau, the highest value of model efficiency was equal to 0.826 and was

obtained with a slope-adjusted and calibrated CN function. Huang et al. (2007) reported a model efficiency of 0.779 by using $\lambda = 0.001$ and a non-linear equation between CN and the soil moisture in the 0–15 cm layer.

4.4 | Effects of Plot Length, Steepness and Soil Moisture on CN

The inverse relation of CN with plot length (Figures 7a and 8a) is somewhat consistent with previous results concerning scale effects on plot runoff at Sparacia. Bagarello and Ferro (2017) applied common regression analysis techniques to fit specific $Q-l$ power relationships to the data recorded at event scale. Even though the scaling effect was predominantly missing, when it was detected, runoff always decreased in longer plots. This scale effect can be explained by run-on processes that enhance infiltration with runoff travel distances but diminish to even become insignificant as rainfall intensity increases (Chen et al. 2016). According to Kidron (2011), contributing areas to runoff in arid zones can mainly be confined to a narrow belt at the bottom of the slope, and scale effects are an inherent outcome of rain properties due to the intermittent character of rain spells. In this perspective, a lower runoff depth is obtained on longer plots because the total runoff volume is averaged across the entire plot area even though it includes a non-contributing and a contributing part. The latter part is nearly constant between different plot lengths while the former has an increasing weight in the runoff calculation for longer plots.

The prevailing direct relationship of CN against plot steepness (Figures 7b and 8b) agrees with the findings by Huang et al. (2006) and Lal et al. (2015). In other words, the present and literature investigations resulted in runoff depths increasing with plot steepness. An increased runoff depth for steeper slopes can be explained by the reduction of the initial abstraction and, in addition, the infiltration due to the decreased travel time of the runoff on the plot (Huang et al. 2006; Lal et al. 2015).

As expected, CN values increased as soil moisture before the rainfall event increased (Figure 11). This implies that the potential maximum retention S decreased for wetter conditions, which is consistent with the result obtained at a small basin scale (3.7 ha) in the Sparacia station, with both satellite and in situ soil moisture measurements (Pampalone et al. 2012). Specifically, the rainfall-runoff data were collected at the basin outlet which is located close to the 22% sloping plots, and the gravimetric soil moisture data were a portion of those used here, that is, related to the period 2004–2009 and to the top 0.05 m of soil and the 0.05–0.10 m layer. In accordance with other studies (Brocca, Melone, Moramarco, Morbidelli 2009; Brocca, Melone, Moramarco, Singh 2009; Trambly et al. 2010) and the physical reason for which S is the initial soil moisture deficit that must be filled to initiate runoff, S decreased as θ increased. The plot investigations by Lal et al. (2015) and Huang et al. (2007) also pointed out the dependence of CN on θ , which was quantitatively expressed by site-specific relationships. The results from basin and plot spatial scales confirm the important role of soil moisture for floods, especially for Mediterranean basins (e.g., Brocca et al. 2008), and runoff from the related source areas, that is, hillslopes.

Neither soil moisture nor soil moisture and event rainfall depth together are effective variables in predicting CN, as only 19% of CN variation for fixed plot length and steepness was explained by these two variables (Equation 10). The further data restriction to a specific erosion component, that is the interrill one, has more than doubled the explained CN variance (41%) (Equation 11) that, however, remains low. Therefore, other factors, besides l , s , θ and P must affect the rainfall-runoff process at plot scale. Possible sources of variability of plot hydrological response are the extent of the time between tillage operations and event (Wendt et al. 1986), and rainfall intensity and duration (Hawkins 1982). Finally, the so-called natural variability (Nearing et al. 1999) produces a within-event unexplained variance of soil loss and runoff measurements in identical plots subjected to the same rainfall. It is an inherent source of runoff variability that tends to decrease as the mean measured value increases, as also demonstrated by Bagarello and Ferro (2010) using data from the 8 m \times 22 m plots established at Sparacia.

4.5 | Accuracy of Soil Loss Estimation by USLE-MB Model With Simulated Runoff

The performance of the USLE-MB model (Equation 1) with the calculated runoff coefficient slightly worsens compared to that with the measured one (Figure 13). The worsening is expected due to the inherent limits of the CN method and, not least, the inability to account for the natural variability of runoff measurements that, instead, is considered when the measured Q_R is used.

This result is indicated by the increased values of the relative standard error in soil loss prediction for the lower and upper rainfall ranges. However, for the lower rainfall range, the use of both the measured and calculated runoff coefficient results in an unsatisfactory performance as USLE-MB works as the measured mean soil loss. Conversely, for the upper rainfall range, the performance of the USLE-MB with the calculated runoff coefficient is fairly satisfactory. The comparison between soil loss estimations reported in Figure 14 shows that data are distributed around the line of perfect agreement, thus indicating a moderate effect on the USLE-MB prediction by using a runoff coefficient calculated by the CN method instead of the measured one. The visual inspection of the scatterplots in Figure 13 reveals a tendency to underestimate the extremely high soil losses ($> 100 \text{ t ha}^{-1}$). The absolute error for these data is, however, acceptable as it ranges from 22% to 43% for the USLE-MB with the measured runoff coefficient and from 18% to 53% for the model applied with the calculated runoff coefficient.

For just over a decade, efforts have been made to incorporate reliable and parsimonious methods for the runoff estimation in the USLE-based models at the plot scale. Gao et al. (2012) coupled a modified SCS-CN and RUSLE model for runoff and soil loss estimations from woodland and grassland plots in the Loess Plateau. The performance of the modified RUSLE model with the simulated runoff coefficient slightly worsened compared to that with the measured runoff coefficient, but NSEI remained over 0.7, which is higher than the NSEI value (0.54) obtained here for the experimental range ($41.6 < P \leq 145.8 \text{ mm}$) where the

combination of USLE-MB and SCS-CN provides satisfactory soil loss predictions. Using data collected from the bare plots of the Masse station (central Italy), Todisco et al. (2015) observed that the accuracy in estimating the event soil loss of the USLE-MM model with the simulated runoff coefficient was slightly higher than that obtained with a model that uses the satellite soil moisture in the erosivity index and slightly lower than that obtained with the same model and a modelled soil moisture. Therefore, it was underlined that the antecedent soil moisture is a good alternative compared to runoff for correcting the rainfall-runoff erosivity index in the USLE-MM model. Shi et al. (2018) proposed a storm-based model, named CSLE, which incorporates a modified SCS-CN. CSLE is a USLE-based model specifically developed for the Loess Plateau. Using runoff and soil loss data from three plots with vegetation cover, the authors obtained a NSEI value of 0.61 for the CLSE with calculated runoff, which is slightly lower than NSEI = 0.65 noted for the CLSE with measured runoff, and close to NSEI = 0.54 obtained in this investigation. They stated that CSLE combined with the SCS-CN can accurately predict soil loss that is normally caused by interrill and rill erosion in the Loess Plateau. Todisco et al. (2022) coupled the USLE-MM and a runoff coefficient estimated by equations based on the integrated use of satellite soil moisture data and event rainfall depth. In particular, using runoff data from the bare plots of the Masse station and surface soil moisture data derived from Copernicus Sentinel-1, they calibrated two regression equations, distinguished by season, of Q against the Antecedent Degree of Saturation Index (ADSI) plus rainfall depth P . They observed a moderate effect on soil loss prediction by using a runoff coefficient calculated by satellite and rainfall data instead of the measured one. The USLE-MM with the estimated Q_R gave a root mean square error of 0.57 t ha^{-1} , which is slightly higher than the value of 0.46 t ha^{-1} obtained with measured Q_R .

Finally, the different studies suggest that incorporating a simulated runoff coefficient in USLE-based models is viable for predicting event soil loss at the plot scale and can enhance the practical interest for these runoff-driven models.

5 | Conclusions

This investigation aimed to calibrate the CN method using rainfall-runoff data observed at the Sparacia experimental station over the last two decades and to investigate the possibility of coupling the simulated runoff and USLE-MB for soil loss estimation. First, the analysis allowed for setting λ to 0.0001 for the study area, which reflects other findings from the literature in which the CN method is applied at the plot scale.

The results inherent to runoff simulation indicated that (i) highest and best reproduced CN values resulted from rill data, (ii) the least squares and median value calibration approaches performed similarly and (iii) the best model fit was systematically produced for rainfall depths less than the median value over the entire monitoring period. Considering the relative standard error, the CN method was suitable only for rill data associated with both rainfall depth under and over the median. However, even in these cases, it performed in an only approximately satisfactory manner.

In accordance with plot literature studies, CN generally increased with plot steepness. Results also showed the need to take the effect of plot length into account, contrary to the original CN model, as CN decreased for increasing values of the plot length. Among the other variables affecting runoff, soil moisture was found to be related to CN but, both individually and coupled with event rainfall depth, it cannot explain the detected CN variability for a given plot type. Therefore, additional factors, including tillage operations, rainfall characteristics, and runoff natural variability, could affect the rainfall-runoff transformation process at the plot scale.

Considering that the inclusion of the measured runoff term in the erosivity factor of the modified versions of the USLE significantly improved soil loss predictions as compared to the USLE, it was then tested if incorporating the modelled runoff in the USLE-MB, which is essential for predictive purposes, allows for maintaining a good model reliability. The test was limited to the events with rill formation as the CN method was suitable in reproducing runoff only for this type of event. The USLE-MB with the calculated runoff coefficient provided satisfactory soil loss predictions although limited to the events characterised by rainfall depths over the median value of the experimental series.

The main limitation of the present investigation is the use of a single land use (cultivated fallow). On the other hand, this condition is common in some periods of the year in the hills of western Sicily planted with wheat.

Future research will be oriented to investigate the applicability of the CN method on vegetated plots of the study area and in other Italian experimental stations for erosion measurements. Finally, further efforts will be directed to test alternative simple methods for plot runoff estimation and their coupled use with USLE-type models.

Acknowledgements

All authors set up the research, analysed and interpreted the results and contributed to write the paper. This study was carried out within the RETURN Extended Partnership and received funding from the European Union Next-GenerationEU (National Recovery and Resilience Plan-NRRP, Mission 4, Component 2, Investment 1.3-D.D. 1243 2/8/2022, PE0000005). This study was also carried out within the PRIN 2022 “Soil Conservation for sustainable Agriculture in the framework of the European green deal” (SCALE), Project code 2022PB2NSP, CUP B53D23017980006 and received funding from the European Union Next-GenerationEU (National Recovery and Resilience Plan-NRRP, Mission 4, Component 2, Investment 1.1). Open access publishing facilitated by Università degli Studi di Palermo, as part of the Wiley - CRUI-CARE agreement.

Data Availability Statement

The data supporting this study's findings are available from the authors upon reasonable request.

References

Assaye, H., J. Nyssen, J. Poesen, et al. 2021. “Curve Number Calibration for Measuring Impacts of Land Management in Sub-Humid Ethiopia.” *Journal of Hydrology: Regional Studies* 35: 100819.

Bagarello, V., G. V. Di Piazza, and V. Ferro. 2004. “Manual Sampling and Tank Size Effects on the Calibration Curve of Plot Sediment Storage Tanks.” *Transactions of ASAE* 47: 1105–1112.

Bagarello, V., G. V. Di Piazza, V. Ferro, and G. Giordano. 2008. “Predicting Unit Plot Soil Loss in Sicily, South Italy.” *Hydrological Processes* 22: 586–595.

Bagarello, V., C. Di Stefano, V. Ferro, and V. Pampalone. 2010a. “Statistical Distribution of Soil Loss and Sediment Yield at Sparacia Experimental Area, Sicily.” *Catena* 82: 45–52.

Bagarello, V., C. Di Stefano, V. Ferro, and V. Pampalone. 2011. “Using Plot Loss Distribution for Soil Conservation Design.” *Catena* 86: 172–177.

Bagarello, V., C. Di Stefano, V. Ferro, and V. Pampalone. 2017. “Predicting Maximum Annual Values of Event Soil Loss by USLE-Type Models.” *Catena* 155: 10–19.

Bagarello, V., C. Di Stefano, V. Ferro, and V. Pampalone. 2018. “Comparing Theoretically Supported Rainfall-Runoff Erosivity Factors at the Sparacia (South Italy) Experimental Site.” *Hydrological Processes* 32: 507–515.

Bagarello, V., and V. Ferro. 2010. “Analysis of Soil Loss Data From Plots of Differing Length for the Sparacia Experimental Area, Sicily, Italy.” *Biosystems Engineering* 105: 411–422.

Bagarello, V., and V. Ferro. 2017. “Scale Effects on Plot Runoff and Soil Erosion in a Mediterranean Environment.” *Vadose Zone Journal* 16: 1–14.

Bagarello, V., V. Ferro, and D. C. Flanagan. 2018. “Predicting Plot Soil Loss by Empirical and Process-Oriented Approaches. A Review.” *Journal of Agricultural Engineering* XLIX: 710.

Bagarello, V., V. Ferro, and G. Giordano. 2010b. “Testing Alternative Erosivity Indices to Predict Event Soil Loss From Bare Plots in Southern Italy.” *Hydrological Processes* 24: 789–797.

Bagarello, V., V. Ferro, G. Giordano, et al. 2011. “Effect of Plot Size on Measured Soil Loss for Two Italian Experimental Sites.” *Biosystems Engineering* 108: 18–27.

Bagarello, V., V. Ferro, and V. Pampalone. 2013. “A New Expression of the Slope Length Factor to Apply USLE-MM at Sparacia Experimental Area (Southern Italy).” *Catena* 102: 21–26.

Bagarello, V., V. Ferro, and V. Pampalone. 2015a. “A New Version of the USLE-MM for Predicting Bare Plot Soil Loss at the Sparacia (South Italy) Experimental Site.” *Hydrological Processes* 29: 4210–4219.

Bagarello, V., V. Ferro, and V. Pampalone. 2015b. “Testing Assumptions and Procedures to Empirically Predict Bare Plot Soil Loss in a Mediterranean Environment.” *Hydrological Processes* 29, no. 10: 2414–2424.

Bagarello, V., V. Ferro, and V. Pampalone. 2020. “A Comprehensive Analysis of Universal Soil Loss Equation Based Models at the Sparacia Experimental Area.” *Hydrological Processes* 34: 1545–1557.

Beasley, D. B., L. F. Huggins, and E. J. Monke. 1980. “ANSWERS: A Model for Watershed Planning.” *Transactions of ASAE* 23: 938–944.

Boardman, J. 2006. “Soil Erosion Science: Reflections on the Limitations of Current Approaches.” *Catena* 68, no. 2–3: 73–86.

Bosznay, M. 1989. “Generalization of SCS Curve Number Method.” *Journal of Irrigation and Drainage Engineering* 115, no. 1: 139–144.

Branson, F. A., G. F. Gifford, K. G. Renard, and R. F. Hadley. 1981. *Rangeland Hydrology*. Society for Range Management, Range Science Series No.1, Kendall/Hunt Pub. Co.

Branson, F. A., R. F. Miller, and I. S. Queen. 1962. “Effects of Contour Furrowing, Grazing Intensities, and Soils on Infiltration Rates, Soil Moisture and Vegetation Near Fort Peck, Montana.” *Journal of Range Management* 15: 151–158.

- Brocca, L., F. Melone, and T. Moramarco. 2008. "On the Estimation of Antecedent Wetness Conditions in Rainfall-Runoff Modelling." *Hydrological Processes* 22: 629–642.
- Brocca, L., F. Melone, T. Moramarco, and R. Morbidelli. 2009. "Antecedent Wetness Conditions Based on ERS Scatterometer Data." *Journal of Hydrology* 364, no. 1–2: 73–87.
- Brocca, L., F. Melone, T. Moramarco, and V. P. Singh. 2009. "Assimilation of Observed Soil Moisture Data in Storm Rainfall-Runoff Modelling." *Journal of Hydrologic Engineering* 14, no. 2: 153–165.
- Cao, L., K. Zhang, H. Dai, and Y. Liang. 2015. "Modeling Interrill Erosion on Unpaved Roads in the Loess Plateau of China." *Land Degradation and Development* 26: 825–832.
- Carollo, F. G., C. Di Stefano, V. Ferro, V. Pampalone, and F. Sanzone. 2016. "Testing a New Sampler for Measuring Plot Soil Loss." *Earth Surface Processes and Landforms* 41: 867–874.
- Carollo, F. G., M. A. Serio, and V. Ferro. 2018. "Predicting Rainfall Erosivity by Momentum and Kinetic Energy in Mediterranean Environment." *Journal of Hydrology* 560: 173–183.
- Chaplot, V., and Y. Le Bissonnais. 2000. "Field Measurement of Interrill Erosion Under Different Slopes and Plot Sizes." *Earth Surface Processes and Landforms* 25: 145–153.
- Chen, L., S. Sela, T. Svoray, and S. Assouline. 2016. "Scale Dependence of Hortonian Rainfall-Runoff Processes in a Semiarid Environment." *Water Resources Research* 52: 5149–5166.
- Chin, D. A. 2023. "Discussion of "NRCS Curve Number Method: Comparison of Methods for Estimating the Curve Number From Rainfall-Runoff Data"." *Journal of Hydrologic Engineering* 28: 07023003.
- Di Stefano, C., V. Pampalone, F. Todisco, L. Vergni, and V. Ferro. 2019. "Testing the Universal Soil Loss Equation-MB Equation in Plots in Central and South Italy." *Hydrological Processes* 33: 2422–2433.
- Edwards, W. M., and L. B. Owens. 1991. "Large Storm Effects on Total Soil Erosion." *Journal of Soil and Water Conservation* 46: 75–78.
- Evert, S. R., and G. R. Dutt. 1985. "Length and Slope Effects on Runoff From Sodium Dispersed, Compacted Earth Microcatchments." *Soil Science Society of America Journal* 49, no. 3: 734–738.
- Ferro, V. 2010. "Deducing the USLE Mathematical Structure by Dimensional Analysis and Self-Similarity Theory." *Biosystems Engineering* 106: 216–220.
- Fu, S., G. Zhang, N. Wang, and L. Luo. 2011. "Initial Abstraction Ratio in the SCS-CN Method in the Loess Plateau of China." *Transactions of the ASABE* 54, no. 1: 163–169.
- Gao, G. Y., B. J. Fu, Y. H. Lü, Y. Liu, S. Wang, and J. Zhou. 2012. "Coupling the Modified SCS-CN and RUSLE Models to Simulate Hydrological Effects of Restoring Vegetation in the Loess Plateau of China." *Hydrology and Earth System Sciences* 16: 2347–2364.
- Gessesse, B., W. Bewket, and A. Bräuning. 2015. "Model-Based Characterization and Monitoring of Runoff and Soil Erosion in Response to Land Use/Land Cover Changes in the Modjo Watershed, Ethiopia." *Land Degradation & Development* 26: 711–724.
- González-Hidalgo, J. C., J. L. Peña-Monné, and M. de Luis. 2007. "A Review of Daily Soil Erosion in Western Mediterranean Areas." *Catena* 71: 193–199.
- Hawkins, R. H. 1978. "Runoff Curve Numbers With Varying Site Moisture." *Journal of the Irrigation and Drainage Division* 104: 389–398.
- Hawkins, R. H. 1982. "Interpretations of Source Area Variability in Rainfall-runoff Relations." In *Proceedings of International Symposium on Rainfall Runoff Modeling*, 303–324. Water Resour. Pub, Littleton, Co.
- Hawkins, R. H., A. T. Hjelmfelt, and A. W. Zevenbergen. 1985. "Runoff Probability, Storm Depth, and Curve Numbers." *Journal of Irrigation and Drainage Engineering* 111, no. 4: 330–340.
- Hawkins, R. H., R. Jiang, D. E. Woodward, A. T. Hjelmfelt, J. A. van Mullem, and Q. D. Quan. 2002. "Runoff Curve Number Method: Examination of the Initial Abstraction Ratio." In *Proceedings of the Second Federal Interagency Hydrologic Modeling Conference*. ASCE Publications.
- Hawkins, R. H., T. J. Ward, D. E. Woodward, and J. A. Van Mullem. 2009. *Curve Number Hydrology—State of the Practice*. ASCE.
- Huang, M., J. Gallichand, C. Dong, Z. Wang, and M. Shao. 2007. "Use of Soil Moisture Data and Curve Number Method for Estimating Runoff in the Loess Plateau of China." *Hydrological Processes* 21, no. 11: 1471–1481.
- Huang, M., G. Jagues, Z. Wang, and G. Monique. 2006. "A Modification to the Soil Conservation Service Curve Number Method for Steep Slopes in the Loess Plateau of China." *Hydrological Processes* 20, no. 3: 579–589.
- Kidron, G. J. 2011. "Runoff Generation and Sediment Yield on Homogeneous Dune Slopes: Scale Effect and Implications for Analysis." *Earth Surface Processes and Landforms* 36: 1809–1824.
- Kinnell, P. I. A. 2007. "Runoff Dependent Erosivity and Slope Length Factors Suitable for Modeling Annual Erosion Using the Universal Soil Loss Equation." *Hydrological Processes* 21: 2681–2689.
- Kinnell, P. I. A. 2010. "Event Soil Loss, Runoff and the Universal Soil Loss Equation Family of Models: A Review." *Journal of Hydrology* 385: 384–397.
- Kinnell, P. I. A. 2019. "A Review of the Science and Logic Associated With Approach Used in the Universal Soil Loss Equation Family of Models." *Soil Systems* 3: 62.
- Kinnell, P. I. A. 2023. "Indices Accounting for Rainstorm Erosivity—Theory and Practice." *Catena* 223: 106925.
- Kinnell, P. I. A., and L. M. Risse. 1998. "USLE-M: Empirical Modeling Rainfall Erosion Through Runoff and Sediment Concentration." *Soil Science Society of America Journal* 62: 1667–1672.
- Knisel, W. G. 1980. *CREAMS: A Field-Scale Model for Chemical, Runoff and Erosion From Agricultural Management Systems, Conservation Research Report*. Vol. 26. South East Area, US Department of Agriculture.
- Lal, M., S. K. Mishra, and A. Pandey. 2015. "Physical Verification of the Effect of Land Features and Antecedent Moisture on Runoff Curve Number." *Catena* 133: 318–327.
- Lal, M., S. K. Mishra, A. Pandey, et al. 2017. "Evaluation of the Soil Conservation Service Curve Number Methodology Using Data From Agricultural Plots." *Hydrogeology Journal* 25, no. 1: 151–167.
- Larson, W. E., M. J. Lindstrom, and T. E. Schumacher. 1997. "The Role of Severe Storms in Soil Erosion: A Problem Needing Consideration." *Journal of Soil and Water Conservation* 52: 90–95.
- Liu, Y., G. Liu, H. Xiao, et al. 2023. "Predicting the Interrill Erosion Rate on Hillslopes Incorporating Soil Aggregate Stability on the Loess Plateau of China." *Journal of Hydrology* 622: 129698.
- Mishra, S. K., P. S. Babu, and V. P. Singh. 2007. "SCS-CN Method Revisited." In *Advances in Hydraulics and Hydrology*. Water Resources Publications.
- Mishra, S. K., R. K. Sahu, T. I. Eldho, and M. K. Jain. 2006. "An Improved Ia-S Relation Incorporating Antecedent Moisture in SCS-CN Methodology." *Water Resources Management* 20, no. 5: 643–660.
- Moglen, G. E., H. Sadeq, L. H. Hughes II, et al. 2022. "NRCS Curve Number Method: Comparison of Methods for Estimating the Curve Number From Rainfall-Runoff Data." *Journal of Hydrologic Engineering* 27: 04022023.
- Moglen, G. E., H. Sadeq, L. H. Hughes II, et al. 2023. "Closure to "NRCS Curve Number Method: Comparison of Methods for Estimating the Curve Number From Rainfall-Runoff Data"." *Journal of Hydrologic Engineering* 28: 07023004.

- Morgan, R. P. C. 2005. *Soil Erosion and Conservation*. 3rd ed. Blackwell.
- Nash, J. E., and J. E. Sutcliffe. 1970. "River Forecasting Through Conceptual Models. Part I—A Discussion of Principles." *Journal of Hydrology* 10: 282–290.
- Nearing, M. A. 2013. "Soil Erosion and Conservation." In *Environmental Modelling: Finding Simplicity in Complexity*, edited by J. Wainwright and M. Mulligan, Second ed., 365–378. John Wiley & Sons, Ltd.
- Nearing, M. A., G. Govers, and L. D. Norton. 1999. "Variability in Soil Erosion Data From Replicated Plots." *Soil Science Society of America Journal* 63: 1829–1835.
- Neitsch, S. L., J. G. Arnold, J. R. Kiniry, and J. R. Williams. 2005. *Soil and Water Assessment Tool Theoretical Documentation*. Texas Water Resources Institute.
- NRCS National Engineering Handbook. 2004a. "Chapter 10 Estimation of Direct Runoff From Storm Rainfall." In *Part 630 Hydrology*. National Resources Conservation Service, USDA.
- NRCS National Engineering Handbook. 2004b. "Chapter 9 Hydrologic Soil-Cover Complexes." In *Part 630 Hydrology*. National Resources Conservation Service, USDA.
- NRCS National Engineering Handbook. 2009. "Chapter 7 Hydrologic Soil Groups." In *Part 630 Hydrology*. National Resources Conservation Service, USDA.
- Pampalone, V., L. Brocca, V. Bagarello, et al. 2012. "Simulazione Dei Deflussi per il Bacino Sperimentale SPA1 di Sparacia." *Quaderni di Idronomia Montana, EdiBios* 30: 363–372 (in Italian with English Abstract).
- Pampalone, V., F. G. Carollo, A. Nicosia, et al. 2022. "Measurement of Water Soil Erosion at Sparacia Experimental Area (Southern Italy): A Summary of More Than Twenty Years of Scientific Activity." *Water* 14: 1881.
- Pampalone, V., C. Di Stefano, and V. Ferro. 2018. "Comment on "Determining Soil Erodibility for the USLE-MM Rainfall Erosion Model by P.I.A. Kinnell, Catena"." *Catena* 167: 440–443.
- Pampalone, V., and V. Ferro. 2020. "Estimating Soil Loss of Given Return Period by USLE-M-Type Models." *Hydrological Processes* 34: 2324–2336.
- Pampalone, V., A. Nicosia, V. Palmeri, M. A. Serio, and V. Ferro. 2023. "Rill and Interrill Soil Loss Estimations by the USLE-MB Equation at the Sparacia Experimental Site (South Italy)." *Water* 15: 2396.
- Ponce, V. M., and R. H. Hawkins. 1996. "Runoff Curve Number: Has It Reached Maturity?" *Journal of Hydrologic Engineering* 1, no. 1: 11–19.
- SCS National Engineering Handbook. 1985. "Section 4: Hydrology." In *Soil Conservation Service*. USDA.
- SCS National Engineering Handbook. 1993. "Section 4: Hydrology, Chapter 4." In *Soil Conservation Service*. USDA.
- Serio, M. A., F. G. Carollo, and V. Ferro. 2019. "A Method for Evaluating Rainfall Kinetic Power by a Characteristic Drop Diameter." *Journal of Hydrology* 577: 123996.
- Sharpley, N., and J. R. Williams, eds. 1990. "EPIC-Erosion Productivity Impact Calculator: 1. Model Documentation." USDA Technical Bulletin. No. 1768.
- Shi, W., M. Huang, and S. L. Barbour. 2018. "Storm-Based CSLE That Incorporates the Estimated Runoff for Soil Loss Prediction on the Chinese Loess Plateau." *Soil and Tillage Research* 180: 137–147.
- Todisco, F., L. Brocca, F. Termiti, and W. Wagner. 2015. "Use of Satellite and Modeled Soil Moisture Data for Predicting Event Soil Loss at the Plot Scale." *Hydrology and Earth System Sciences* 19: 3845–3856.
- Todisco, F., L. Vergni, S. Ortenzi, and L. Di Matteo. 2022. "Soil Loss Estimation Coupling a Modified USLE Model With a Runoff Correction Factor Based on Rainfall and Satellite Soil Moisture Data." *Water* 14: 2081.
- Tramblay, Y., C. Bouvier, C. Martin, J. F. Didon-Lescot, D. Todorovik, and J. M. Domergue. 2010. "Assessment of Initial Soil Moisture Conditions for Event-Based Rainfall–Runoff Modelling." *Journal of Hydrology* 387, no. 3–4: 176–187.
- Vandervaere, J. P., M. Vauclin, R. Haverkamp, C. Peugeot, J. L. Thony, and M. Gilfedder. 1998. "Prediction of Crust-Induced Surface Runoff With Disc Infiltrometer Data." *Soil Science* 163: 9–21.
- Wendt, R. C., E. E. Alberts, and A. T. Hjelmfelt Jr. 1986. "Variability of Runoff and Soil Loss From Fallow Experimental Plots." *Soil Science Society of America Journal* 50: 730–736.
- Wischmeier, W. H., and D. D. Smith. 1978. "Predicting Rainfall-Erosion Losses—A Guide to Conservation Farming." In *USDA Agriculture Handbook*, 537. U.S. Department of Agriculture.
- Young, R. A., C. A. Onstad, D. D. Bosch, and W. P. Anderson. 1989. "AGNPS: A Nonpoint-Source Pollution Model for Evaluating Agricultural Watersheds." *Journal of Soil and Water Conservation* 44: 168–173.
- Yu, B., C. W. Rose, K. J. Coughlan, and B. Fentie. 1997. "Plot-Scale Rainfall-Runoff Characteristics and Modeling at Six Sites in Australia and Southeast Asia." *Transactions of ASAE* 40, no. 5: 1295–1303.

Supporting Information

Additional supporting information can be found online in the Supporting Information section.